IAA24 are likely participants in auxin gene regulation through the TGTCTC elements. A single copy of ER8 was a more active AuxRE than other constructs that contained two copies of TGTCTC (*3*, *11*) and could represent the perfect palindromic AuxRE, similar to the perfect palindromic GRE (*4*).

As the COOH-terminal βαα-motif has no apparent effect on ARF1 binding to DNA, what might be its function? We used the COOH-terminal region of ARF1 as bait in a yeast two-hybrid screen (*14*) and isolated two identical cDNA clones from an *Arabidopsis* cDNA expression library. The translated open reading frame encoded a protein (ARF1-Binding Protein or ARF1-BP) that contained a region with amino acid sequence similarity to boxes III and IV of ARF1 (Fig. 2, A and C). ARF1-BP showed less similarity to boxes III and IV in Aux/IAA and IAA24 proteins. Thus, boxes III and IV in ARF1 may facilitate interaction of ARF1 with ARF1-BP, and these interactions may contribute to auxin responsiveness.

Genetic approaches to dissect the auxin signal transduction pathway have resulted in the cloning of *AXR1*, *AUX1*, and *hookless1* genes (*15*). Identification of the relevant transcription factors should facilitate elucidation of the mechanisms involved in auxin-regulated gene expression.

REFERENCES AND NOTES

1. S. Abel and A. Theologis, *Plant Physiol.* **111**, 9 (1996).
2. T. J. Guilfoyle *et al.*, *Aust. J. Plant Physiol.* **20**, 489 (1993); Z.-B. Liu, T. Ulmasov, X. Shi, G. Hagen, T. J. Guilfoyle, *Plant Cell* **6**, 645 (1994).
3. T. Ulmasov, Z.-B. Liu, G. Hagen, T. J. Guilfoyle, *Plant Cell* **7**, 1611 (1995).
4. K. R. Yamamoto, D. Pearce, J. Thomas, J. N. Miner, in *Transcriptional Regulation*, S. L. McKnight, K. R. Yamamoto, Eds. (Cold Spring Harbor Laboratory Press, Plainview, NY, 1992), pp. 1169–1192.
5. The P3(4×) AuxRE was placed upstream of the minimal promoter in pHISi-1 and pLacZi vectors (MATCHMAKER One-Hybrid System; Clontech). These vectors were linearized and sequentially transformed into the yeast strain Y4271 (Clontech). Background LacZ activity in late logarithmic-phase cells for the engineered strain Y4271::P3(4×) was higher than for the pLacZi vector (no AuxREs) but low enough to distinguish from a positive interaction. Low plating density (10^8 cells per 150-mm plate) and 3-aminotriazole (3-AT; 45 mM) were used to suppress growth on histidine-deficient (−His) plates resulting from the low amount of P3(4×)-HIS3 reporter gene expression. An *Arabidopsis* cDNA expression library cloned into the GAL4 activation domain vector pGAD10 (Clontech) was amplified in *Escherichia coli*. Purified library DNA (500 μg) was used to transform the Y4271::P3(4×) strain. Of 1.2×10^8 transformants, 500 colonies grew on −His plates containing 3-AT, and these were screened for lacZ activity. LacZ-positive colonies (212) were selected, and library plasmids were isolated. Sizes of the cDNA inserts were determined by polymerase chain reaction (PCR) with primers that flanked the cDNA inserts. Plasmids harboring different-sized inserts were rescued by transformation into *E. coli* and retransformed into the Y4271::P3(4×) strain. Clones that restored lacZ activity were sequenced, and five clones encoding ARF1 were recovered.
6. An ARF3 cDNA (GenBank accession number U89926) was isolated from the MATCHMAKER cDNA library by using an unannotated *Arabidopsis* sequence (GenBank accession number U78721) related to the NH_2-terminal region of ARF1.
7. D. R. McCarty *et al.*, *Cell* **66**, 895 (1991).
8. J. Giraudat *et al. Plant Cell* **4**, 1251 (1992).
9. S. Abel, P. W. Oeller, A. Theologis, *Proc. Natl. Acad. Sci. U.S.A.* **91**, 326 (1994).
10. S. J. Treizenberg, *Curr. Biol.* **5**, 190 (1995).
11. T. Ulmasov and G. Hagen, unpublished results.
12. N. Ballas, L.-M. Wong, K. Malcolm, A. Theologis, *Proc. Natl. Acad. Sci. U.S.A.* **92**, 3483 (1995).
13. The ER0 spacing construct was actTGTCTCGAGACAac. ER1 to ER9 contained spacers between actTGTCTC and GAGACAac of one to nine nucleotides: a, aa, cag, caag, ccagg, ccaagg, ccaaagg, ccattagg, and ccatttagg.
14. The COOH-terminus of ARF1 [amino acids (aa) 533 to 665] served as bait to screen the library used in the one-hybrid screen. The interacting clone encoded the COOH-terminal portion of ARF1-BP (aa 273 to 410). Complementary DNA clones encoding NH_2-terminal regions of ARF1-BP cDNA were isolated by PCR.
15. H. M. Leyser *et al.*, *Nature* **364**, 161 (1993); M. J. Bennett *et al.*, *Science* **273**, 948 (1996); A. Lehman, R. Black, J. R. Ecker, *Cell* **85**, 183 (1996).
16. F. Ausubel *et al.*, Eds., *Current Protocols in Molecular Biology* (Wiley, New York, 1995).
17. Abbreviations for the amino acid residues are: A, Ala; C, Cys; D, Asp; E, Glu; F, Phe; G, Gly; H, His; I, Ile; K, Lys; L, Leu; M, Met; N, Asn; P, Pro; Q, Gln; R, Arg; S, Ser; T, Thr; V, Val; W, Trp; and Y, Tyr.
18. Histidine-tagged ARF1 was expressed and purified from *E. coli*, full-length and truncated forms of ARF1 were synthesized in vitro in FlexiRabbit reticulocyte lysates (Promega), and gel-shift assays were done as described (*16*).
19. The IAA24 ORF was isolated from the MATCHMAKER cDNA library by PCR. IAA24 protein was produced by in vitro translation.

20. Supported by NSF grants IBN 9303956 and MCB 9604208. We thank W. Yu and X. Feng for technical assistance.

25 February 1997; accepted 24 April 1997

Large Porous Particles for Pulmonary Drug Delivery

David A. Edwards,* Justin Hanes, Giovanni Caponetti, Jeffrey Hrkach, Abdelaziz Ben-Jebria, Mary Lou Eskew, Jeffrey Mintzes, Daniel Deaver, Noah Lotan, Robert Langer*

A new type of inhalation aerosol, characterized by particles of small mass density and large size, permitted the highly efficient delivery of inhaled therapeutics into the systemic circulation. Particles with mass densities less than 0.4 gram per cubic centimeter and mean diameters exceeding 5 micrometers were inspired deep into the lungs and escaped the lungs' natural clearance mechanisms until the inhaled particles delivered their therapeutic payload. Inhalation of large porous insulin particles resulted in elevated systemic levels of insulin and suppressed systemic glucose levels for 96 hours, whereas small nonporous insulin particles had this effect for only 4 hours. High systemic bioavailability of testosterone was also achieved by inhalation delivery of porous particles with a mean diameter (20 micrometers) approximately 10 times that of conventional inhaled therapeutic particles.

Inhaled aerosols are effective therapeutic carriers for the treatment of respiratory inflammation (*1*), cystic fibrosis (*2*), and other lung disorders (*3*); they also offer potential for noninvasive systemic delivery of peptides and proteins (*4*). Local and systemic inhalation therapies can often benefit from a controlled release of the therapeutic agent (*5*), as is achievable with the use of biodegradable polymeric materials (*6*). Slow release from an inhaled therapeutic particle can prolong the residence of an administered drug in the airways or acini and can diminish the rate of a drug's appearance in the bloodstream (*7*). Also, patient compliance increases when dosage frequency is reduced (*7*).

The human lungs, however, have efficient means of removing deposited particles over periods ranging from minutes to hours. In the upper airways, ciliated epithelia contribute to the "mucociliary escalator" (*8*), by which particles are swept from the airways toward the mouth. In the deep lungs, an army of alveolar macrophages is capable of phagocytosing particles soon after their deposition (*9*). An effective slow-release inhalation therapy therefore requires a means of avoiding or suspend-

D. A. Edwards, A. Ben-Jebria, J. Mintzes, Department of Chemical Engineering, Pennsylvania State University, 204 Fenske Laboratory, University Park, PA 16802, USA.
J. Hanes, J. Hrkach, R. Langer, Department of Chemical Engineering, Massachusetts Institute of Technology, Cambridge, MA 02139, USA.
G. Caponetti, Department of Chemical Engineering, Massachusetts Institute of Technology, Cambridge, MA 02139, USA, and Department of Pharmacy, Universite di Parma, 43100 Parma, Italy.
M. L. Eskew, Environmental Resources Research Institute, Pennsylvania State University, Fenske Laboratory, University Park, PA 16802, USA.
D. Deaver, Department of Animal Science, Pennsylvania State University, 324 Henning Building, University Park, PA 16802, USA.
N. Lotan, Department of Biomedical Engineering, Technion–Israel Institute of Technology, Haifa 32000, Israel.

*To whom correspondence should be addressed. E-mail: dxe11@psuv.edu (D.A.E.), rlanger@mit.edu (R.L.).

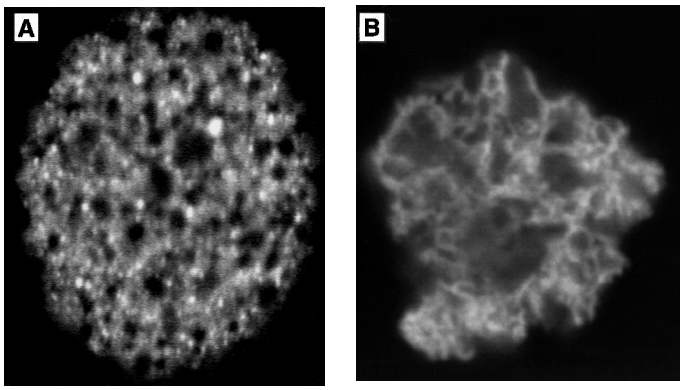

Fig. 1. Confocal microscopy images of (**A**) porous PLGA and (**B**) porous PLAL-Lys particles. Fluorescein isothiocyanate–dextran was encapsulated in the PLGA particle to render the pore spaces of the particle visible in the fluorescent confocal image. The PLAL-Lys particles were fluorescently labeled through the reaction of rhodamine isothiocyanate with lysine amine groups on the surface of the particles. The PLGA and PLAL-Lys particles are highly porous, as evidenced by the appearance of fluorescence throughout the particle structure.

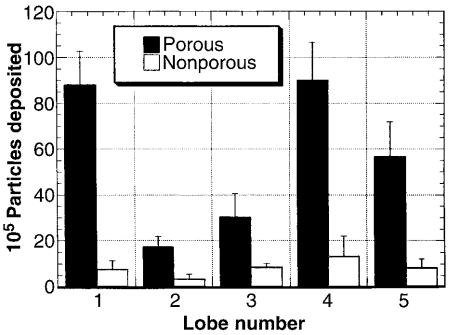

Fig. 2. Total particle recovery in rat lungs after bronchoalveolar lavage. Lobe numbers correspond to (1) left lung, (2) anterior, (3) median, (4) posterior, and (5) postcaval. For porous PLAL-Lys particles, $d = 6.9 \pm 4.2$ μm and $\rho = 0.1$ g/cm^3. For nonporous PLA particles, $d = 6.7 \pm 3.2$ μm and $\rho = 0.94$ g/cm^3. Means and SEs are based on $n = 4$.

ing the lungs' natural clearance mechanisms until encapsulated drugs have been effectively delivered.

Until now, therapeutic dry powder aerosols have been made with particle mass densities (ρ) of $\sim 1 \pm 0.5$ g/cm^3 and mean geometric diameters (d) of <5 μm to avoid excessive deposition in the dry powder inhaler (DPI) and oropharyngeal cavity (*5, 10*). Here, we show that very light particles ($\rho < \sim 0.4$ g/cm^3) with $d > 5$ μm can be deposited in the lungs. As a consequence of their large size and low mass density, porous particles can aerosolize from a DPI more efficiently than smaller nonporous particles, resulting in higher respirable fractions of inhaled therapeutics. Also by virtue of their size, large particles can avoid phagocytic clearance from the lungs until the particles have delivered their therapeutic dose; this attribute can be particularly useful for controlled-release inhalation therapies.

To assess the merits of large porous particles for pulmonary drug delivery, we encapsulated model therapeutics inside porous particles (Fig. 1A) composed of 50:50 poly(lactic acid-*co*-glycolic acid) (PLGA). Double- and single-emulsion solvent evaporation techniques (*11*) were used to prepare porous and nonporous PLGA particles, respectively. Porous and nonporous particles of similar aerodynamic diameter (*12*), loaded with ~15 weight % model therapeutic (testosterone), were aerosolized into a cascade impactor system (*13*) from a Spinhaler DPI for 30 s at an airflow rate of 28.3 liter/min. The cascade impactor provides an in vitro system for estimating the respirable fraction of a dry powder; it consists of a closed chamber within which flat plates are arranged perpendicular to the airflow, such that particles deposit stagewise in a manner reflective of their aerodynamic diameters. After deposition on the stages of the impactor, particles were collected (*13*) and total particle mass was assessed stagewise; the respirable fraction was determined as the percent of total particle mass exiting the DPI, recovered from the terminal, "respirable" stages of the impactor. Nonporous particles [$d = 3.5$ μm, $\rho = 0.8$ g/cm^3 (*14*)] exhibited a respirable fraction of $20.5 \pm 3.5\%$, whereas $50 \pm 10\%$ of porous particles ($d = 8.5$ μm, $\rho = 0.1$ g/cm^3) were respirable, even though the aerodynamic diameters (*12*) of the two particle types are nearly identical. The large porous particles' high efficiency can be attributed to their smaller surface-to-volume ratio. Large particles aggregate less than small particles, all other considerations being equal (*15, 16*); thus, while both have identical aerodynamic diameters, the large particles tend to exit the DPI more generally as single particles. The smaller particles aggregate more, leading to their deposition by gravity and inertia before reaching the "respirable" stages of the impactor.

To assess the influence of particle composition, we aerosolized a second type of porous particle (Fig. 1B), composed of poly(lactic acid-*co*-lysine-*graft*-lysine) (PLAL-Lys) (*11*). The PLAL-Lys particles exhibit some hygroscopicity, possibly a result of their lysine content, whereas the PLGA particles do not. Porous PLAL-Lys aerosols ($d = 8.2$ μm, $\rho < 0.1$ g/cm^3) exhibited an in vitro respirable fraction ($57 \pm 1.9\%$) similar to that of the porous PLGA particles ($50 \pm 10\%$), which suggests that absolute particle mass density, rather than particle chemistry or hygroscopicity, is the prime determinant of the relatively high respirable fractions observed for the large porous particles. The values of $50 \pm 10\%$ and $57 \pm 1.9\%$ for porous particles exceed comparable respirable fractions obtained in recent aerosolization studies (*15*) performed with mannitol ($4 \pm 0.3\%$) and recombinant human granulocyte colony-stimulating factor (blended with mannitol) ($34 \pm 2\%$) powders using a Spinhaler DPI at a similar airflow rate (30 liter/min).

To determine whether the relatively efficient in vitro aerosolization of large porous particles translates into improved respirable fractions in vivo, we aerosolized porous and nonporous particles into the airways of rats (*17*). During forced ventilation, rats were exposed to porous or nonporous particles; bronchoalveolar lavage was used to collect particles deposited in the trachea as well as in the airways and acini (*18*). The nonporous particles deposited primarily in the trachea (~79% of all particle mass that entered the trachea), whereas only 46% of the porous particle mass deposited in the trachea. Particles remaining in the rat lungs after bronchoalveolar lavage were obtained by careful dissection of the individual lobes of the lungs in subsequent experiments (*19*) (Fig. 2). The absolute number of porous particles remaining in the lungs was approximately an order of magnitude greater than the corresponding number of nonporous particles.

The role of low mass density in rendering large particles respirable can be understood in terms of the particles' mean aerodynamic diameter (*12*). Relatively large particles with high porosity have the same aerodynamic diameter as smaller, nonporous particles; these larger particles can enter the lungs because particle mass dictates the location of aerosol deposition in the lungs. The increased aerosolization efficiency of large, light particles lowers the probability of deposition losses before particle entry into the airways, thereby increasing the systemic bioavailability of an inhaled drug.

To test whether large particle size can increase systemic bioavailability, we encapsulated insulin into porous and nonporous polymeric particles. We designed the mass densities and mean diameters of the two particles such that they each had an aerodynamic diameter (~2 μm) suitable for deep lung deposition (*12*); the mean diameters of the porous and nonporous particles were >5 μm and <5 μm, respectively (Fig. 3, A to C). Identical masses of the porous or nonporous particles were administered to rats as an inhalation aerosol or injected subcutaneously (controls)

(*20*). Serum insulin concentrations were monitored as a function of time after inhalation or injection. For both porous (Fig. 3A) and nonporous (Fig. 3B) particles, blood levels of insulin reached high values within the first hour after inhalation. Only with large porous particles did blood levels of insulin remain elevated ($P < 0.05$) beyond 4 hours, with a relatively constant insulin release continuing to at least 96 hours ($0.04 < P < 0.2$). These results were confirmed by serum glucose values (Fig. 3C), which show falling glucose levels for the first 10 hours after inhalation of the porous insulin particles, followed by relatively constant low glucose levels for the remainder of the 96-hour period [for small nonporous insulin particles, initially suppressed glucose values rose after 24 hours (*21*)]. Similar biphasic release profiles of macromolecules from PLGA polymers have been reported (*22*). For the large porous particles, insulin bioavailability relative to subcutaneous injection (*23*) was 87.5%, whereas the small nonporous particles yielded a relative bioavailability of 12% after inhalation. By comparison, bioavailability (relative to subcutaneous injection) of insulin administered to rats as an inhalation liquid aerosol has been reported as 37.3% using a similar endotracheal method (*24*). The absolute bioavailability of insulin inhaled into rat lungs in the form of a lactose-insulin powder through a DPI connected to an endotracheal tube has been reported as 6.5% (*25*). The longest sustained insulin release previously reported (6 hours) was achieved using liposomes intratracheally instilled into rat lungs (*26*).

Given the short systemic half-life of insulin (11 min) (*27*) and the 12- to 24-hour time scale of particle clearance from the central and upper airways (*5*), the appearance of exogenous insulin in the bloodstream several days after inhalation appears to indicate that large porous particles achieve long, nonphagocytosed lifetimes in the deep lungs. To test this hypothesis, we lavaged (*18*) the lungs of rats immediately after inhalation of the porous and nonporous insulin particles as well as 48 hours after inhalation. For nonporous particles, 30 ± 3% of phagocytic cells contained particles immediately after inhalation, and 39 ± 5% contained particles 48 hours after inhalation. By contrast, only 8 ± 2% of phagocytic cells contained large porous particles immediately after inhalation, and 12.5 ± 3.5% contained particles 48 hours after inhalation. For small nonporous particles, 17.5 ± 1.5% of the phagocytic cell population contained three or more particles 48 hours after inhalation, compared with 4 ± 1% for large nonporous particles. Inflammatory response was also elevated with small nonporous particles; neutrophils represented 34 ± 12% of the phagocytic cell population 48 hours after inhalation of the small nonporous particles, compared with 8.5 ± 3.5% for large porous particles (alveolar macrophages represented 100% of cells measured immediately after inhalation). These results are consistent with those of in vitro experiments showing that phagocytosis of particles diminishes precipitously as particle diameter increases beyond 3 μm (*28*).

To further determine whether increased bioavailability correlates with increasing size of porous particles, we encapsulated a second model drug, testosterone, in porous particles of two different mean geometric diameters (10.1 and 20.4 μm). An identical mass of powder was administered to rats as an inhalation aerosol or as a subcutaneous injection (controls). Serum testosterone concentrations were monitored as a function of time after inhalation or injection (Fig. 3, D and E). Blood levels of testosterone remained well above background levels ($P < 0.05$) for 12 to 24 hours, even though the systemic half-life of testosterone is 10 to 20 min (*27*). Testosterone bioavailability relative to subcutaneous injection was 177% for the 20.4-μm-diameter particles (Fig. 3D) and 53% for the 10.1-μm-diameter particles (Fig. 3E). The increase in testosterone bioavailability with increasing size of porous particles is especially notable given that the mean diameter of the 20.4-μm particles is ~10 times that of nonporous conventional therapeutic particles (*5, 10*). The relatively short time scale of testosterone release observed for both the inhalation and subcutaneous controls is near the in vitro time scale of release (several hours) reported elsewhere for 50:50 PLGA microparticles of similar size encapsulating a therapeutic substance (bupivacaine) of similar molecular weight and lipophilicity (*29*).

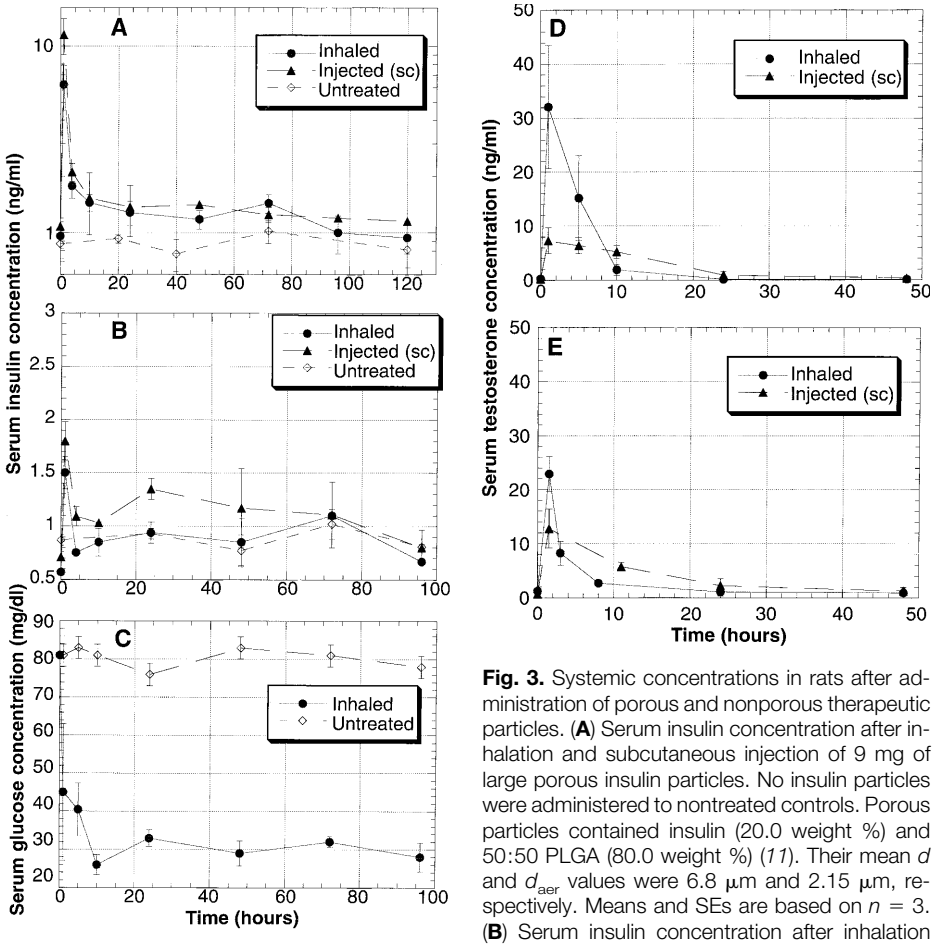

Fig. 3. Systemic concentrations in rats after administration of porous and nonporous therapeutic particles. (**A**) Serum insulin concentration after inhalation and subcutaneous injection of 9 mg of large porous insulin particles. No insulin particles were administered to nontreated controls. Porous particles contained insulin (20.0 weight %) and 50:50 PLGA (80.0 weight %) (*11*). Their mean d and d_{aer} values were 6.8 μm and 2.15 μm, respectively. Means and SEs are based on $n = 3$. (**B**) Serum insulin concentration after inhalation and subcutaneous injection of 9 mg of small nonporous insulin particles. No insulin particles were administered to nontreated controls. Nonporous particles contained insulin (10.0 weight %) and 50:50 PLGA (90.0 weight %) (*11*). Their mean d and d_{aer} values were 4.4 μm and 2.15 μm, respectively. Means and SEs are based on $n = 3$. (**C**) Serum glucose concentration after inhalation of 9 mg of large porous insulin particles or 9 mg of small nonporous insulin particles. No insulin particles were administered to nontreated controls. Means and SEs are based on $n = 3$. (**D**) Serum testosterone concentration after administration of 6 mg of porous testosterone particles ($d = 20.4$ μm) as an inhalation powder and as a subcutaneous control. Particles contained testosterone (15 weight %), 50:50 PLGA (76.5 weight %), and PLAL-Lys (8.5 weight %). For the dry powder, $\rho = 0.1$ g/cm^3. (**E**) Same as (D) but with smaller porous testosterone particles ($d = 10.1$ μm).

Porous particles comprising therapeutics and pharmaceutical excipients can easily be formed by spray-drying (*30*), rapid expansion of supercritical fluids (*31*), and other particle formation technologies. Hence, they can immediately address a variety of needs as therapeutic carriers for inhalation therapies. Their potential for high aerosolization efficiency, long-term drug release, and increased systemic bioavailability makes large porous particles especially attractive for systemic inhalation therapies.

REFERENCES AND NOTES

1. O. Einarsson *et al*., *Ann. N.Y. Acad. Sci.* **762**, 89 (1995).
2. R. Niven, *Crit. Rev. Ther. Drug Carrier Syst.* **12**, 151 (1995).
3. S. J. Smith and J. A. Bernstein, in *Inhalation Aerosols*, A. J. Hickey, Ed. (Dekker, New York, 1996), pp. 233–269.
4. J. S. Patton and R. M. Platz, *Adv. Drug Delivery Rev.* **8**, 179 (1992).
5. I. Gonda, in *Topics in Pharmaceutical Sciences 1991*, D. J. A. Crommelin and K. K. Midha, Eds. (Medpharm Scientific, Stuttgart, 1992), pp. 95–115.
6. R. Langer, *Science* **249**, 1527 (1990).
7. I. Gonda, *Crit. Rev. Ther. Drug Carrier Syst.* **6**, 4273 (1990).
8. D. Pavia, in *Aerosols and the Lung: Clinical and Experimental Aspects*, S. W. Clarke and D. Pavia, Eds. (Butterworths, London, 1984), pp. 200–229.
9. M. B. Warheit and M. A. Hartsky, *Microscopy Res. Tech.* **26**, 412 (1993); J. D. Brain, in *The Reticuloendothelial System*, S. M. Reichard and J. Filkins, Eds. (Plenum, New York, 1985), pp. 315–331.
10. D. Ganderton, *J. Biopharm. Sci.* **3**, 101 (1992); A. Adjei and J. Garren, *Pharm. Res*. **7**, 565 (1990).
11. PLGA particles were made using the double- and single-emulsification solvent evaporation procedures. In the double-emulsification procedure, 300 μl of an aqueous solution was emulsified on ice into 4.0 ml of 50:50 PLGA polymer solution in methylene chloride (200 mg of polymer) by probe sonication. The first emulsion was poured into 100 ml of 1% aqueous polyvinyl alcohol (PVA) solution (average molecular weight 25 kD, 88% hydrolyzed) and homogenized (Silverson Machines, London, England) at 6000 rpm to form the double emulsion. The microspheres were continuously stirred for 3 hours to allow hardening, collected by centrifugation, washed several times with double-distilled water, and freeze-dried into a freely flowing powder. Particles (PLGA or blends of PLGA and PLAL-LYS) containing testosterone were made by dissolving the testosterone in the polymer solution. For the insulin particles, an aqueous solution of human insulin was emulsified with PLGA in the first emulsification. The amounts of water and insulin were decreased to diminish particle porosity, whereas insulin microsphere aerosolization efficiency was enhanced by the addition of L-α-phosphatidylcholine dipalmitoyl to the polymer solution [J. Hanes, thesis, Massachusetts Institute of Technology (1996)]. In the single-emulsification method, 200 mg of the copolymer 50:50 PLGA was dissolved in 2.8 ml of methylene chloride. The polymer solution was homogenized at 7500 rpm in 100 ml of 1% (w/v) aqueous PVA solution. The resulting dispersion was stirred using a magnetic stirrer for 3 hours until the methylene chloride was completely evaporated and the particles hardened. The particles were then isolated by centrifugation. The precipitate was washed three times with distilled water. Finally, the particles were freeze-dried (Labconco freeze dryer 8) for at least 48 hours. Particle sizing was performed using a Coulter Multisizer II (Coulter Electronics, Luton, England). PLGA particles prepared by the single-emulsification method are naturally less porous than those made by double emulsification. For example, PLGA microspheres with bulk mass densities as low as 0.05 g/cm^3 have been prepared by the double-emulsification technique [R. Jeyanthi, B. C. Thanoo, R. C. Metha, P. P. DeLuca, *J. Controlled Release* **38**, 235 (1996)], although these microspheres, at 35 to 140 μm, were inappropriately large for deep-lung inhalation. PLAL-Lys particles were also made using the single-emulsification technique [J. S. Hrkach, J. Ou, N. Lotan, R. Langer, *Macromolecules* **28**, 4736 (1995)]; these particles, apparently because of the cationic charge of the graft copolymer, are highly porous even when prepared by the single-emulsification method.
12. The aerodynamic diameter d_{aer} is related to the actual sphere diameter d by the formula

$$d_{aer} = d\sqrt{\rho} \quad (1)$$

(*5*). Maximal deposition of monodisperse aerosol particles in the alveolar region of the human lung (~60% of the inhaled particles) occurs for d_{aer} = ~3 μm (*32*). Inhaled particles with $d_{aer} > 3$ μm tend to deposit in the upper airways by gravity and inertia, whereas particles with $d_{aer} < 3$ μm tend to be exhaled. On the basis of Eq. 1, the actual diameter d (in micrometers) of porous particles that will exhibit maximum deep-lung deposition because of their small ρ is

$$d = 3/\sqrt{\rho} \quad (2)$$

(where $\rho < 1$). Hence, for such particles d is always greater than 3 μm. For example, porous particles with d = 8.5 μm and ρ = 0.1 g/cm^3 have approximately the same aerodynamic diameter (~2.7 μm) as nonporous particles with d = 3.5 μm and ρ = 0.8 g/cm^3.
13. We placed 20 mg of porous or nonporous microparticles, with encapsulated rhodamine as a fluorescent marker, in No. 1 hard gelatin capsules (Eli Lilly), loaded the capsules into a Spinhaler DPI (Fisons, Bedford, MA), and activated the DPI. Particles were aerosolized into a Mark I Andersen Impactor (Andersen Samplers, Atlanta, GA) from the Spinhaler device for 30 s at a flow rate of 28.3 liter/min. [Each plate of the impactor was previously coated with Tween 80 by immersing the plates in an acetone solution (5% w/v) and then evaporating the acetone in an oven at 60°C for 5 min.] After aerosolization and deposition, particles were collected from each stage of the impactor system and completely degraded in NaOH solution (0.2 N). After incubation at 37°C for 12 hours, the fluorescence of each solution was measured (wavelengths of 554 nm excitation, 574 nm emission).
14. Particle mass density was determined either by nonmercury porosimetry or tap density measurements (Micromeritics, Norcross, GA). The mass density of nonporous particles ranged from ~0.4 to 1.0 g/cm^3. The lower mass density limit (0.4 g/cm^3) is near that recently reported for spray-dried pharmaceutical powders (*15*), whereas the upper limit (1.0 g/cm^3) is similar to the mass density of liquid pharmaceutical aerosols [A. Adjei *et al*., *Int. J. Pharm.* **107**, 57 (1994)] and other dry-powder aerosols [M. T. Vidgren, P. A. Vidgren, T. P. Paronen, *ibid.* **35**, 139 (1987)]. The mass density of porous particles was typically near or equal to 0.1 g/cm^3. Mass density variation from particle to particle within powders did not appear to introduce a substantial source of uncertainty. For example, using an API aerosizer, we measured the mean time-of-flight of the porous and nonporous particles described in the legend of Fig. 2. This gave a mean d_{aer} of 1.57 ± 2.41 μm for the porous particles and 5.82 ± 1.86 μm for the nonporous particles. Using Eq. 1 in (*12*), this indirectly yields a mass density ratio (porous to nonporous) of 0.1 ± 0.3. Given that the measured ratio of mass densities is 0.11 (Fig. 2), mass density variation within the two powders appears to be small (<10%).
15. D. L. French, D. A. Edwards, R. W. Niven, *J. Aerosol Sci*. **27**, 769 (1996).
16. W. I. Li *et al*., *ibid.*, p. 1269.
17. Male Sprague-Dawley rats (150 to 200 g) were anesthetized using ketamine (90 mg/kg)-xylazine (10 mg/kg). Anesthetized rats were placed ventral side up on a surgical table provided with a temperature-controlled pad to maintain physiological temperature. Rats were cannulated above the carina with an endotracheal tube connected to a Harvard ventilator and were force-ventilated for 20 min at 300 ml/min. Fifty micrograms of porous (PLAL-Lys) or nonporous (PLA) microparticles were introduced into the endotracheal tube. After the period of forced ventilation, rats were killed and the lungs and trachea were separately washed using bronchoalveolar lavage (*18*). The lavage fluid was centrifuged (400*g*), and the pellets were collected and resuspended in 2 ml of phenol red–free Hanks' balanced salt solution (HBSS) (Gibco) without Ca^{2+} and Mg^{2+}. A 100-μl sample was removed for particle counting using a hemacytometer. The remaining solution was mixed with 10 ml of 0.4 N NaOH. After incubation at 37°C for 12 hours, the fluorescence of each solution was measured (wavelengths of 554 nm excitation, 574 nm emission).
18. Lungs were lavaged immediately (5 to 10 min) after inhalation. A tracheal cannula was inserted and tied into place, and the airways were washed with 10-ml aliquots of HBSS. The lavage procedure was repeated until a total volume of 30 ml was collected. In the phagocytic cell experiments, lavage fluid was centrifuged and the cell pellets were resuspended in HBSS for counting, differentiation of cell types, and measurement of phagocytosis. Engulfment of particles by phagocytic cells was determined by counting microscopically the number of particles incorporated per cell in wet mounts and in fixed and stained cytocentrifuge preparations. Reported numbers are based on the wet-mount experiments; similar numbers were obtained using the stained cytocentrifuge preparations.
19. The lobes were placed in separate petri dishes containing 5 ml of HBSS. Each lobe was teased through a 60-mesh screen to dissociate the tissue and was then filtered through cotton gauze to remove tissue debris and connective tissue. The petri dish and gauze were washed with an additional 15 ml of HBSS to maximize microparticle collection. Each tissue preparation was centrifuged and resuspended in 2 ml of HBSS, and the particles were counted in a hemacytometer.
20. Rats were anesthetized and cannulated as described (*17*) and were force-ventilated for 10 to 20 min at 300 ml/min. Rats received two types of aerosols through the endotracheal tube. After the period of forced ventilation, necks were sutured and rats were revived within 1 to 2 hours. Blood samples (300 μl) were periodically withdrawn from the tail vein over a period of 2 to 6 days. These samples were mixed with assay buffer, centrifuged, and the supernatant examined for the presence of (endogenous and exogenous) insulin or testosterone using radioimmunoassays (ICN Pharmaceuticals, Costa Mesa, CA). Glucose was measured using a colorimetric assay (Sigma). Control studies involved subcutaneous injection of the same amount of powder as was inhaled. The particles were injected into the scruff of the neck.
21. D. A. Edwards, A. Ben-Jebria, J. Mintzes, J. Hanes, J. Hrkach, R. Langer, G. Caponetti, M. L. Eskew, D. Deaver, N. Lotan, data not shown.
22. S. Cohen *et al*., *Pharm. Res.* **8**, 713 (1991).
23. Bioavailability was determined as $(AUC_{inhaled}/AUC_{subcutaneous}) \times 100$, where AUC is area under the curve.
24. P. Colthorpe *et al*., *Pharm. Res.* **9**, 764 (1992).
25. F. Komada *et al*., *J. Pharm. Sci.* **83**, 863 (1994).
26. F. Y. Liu, Z. Shao, D. O. Kildsig, A. K. Mitra, *Pharm. Res.* **10**, 228 (1993).
27. A. R. Gennaro, Ed., *Remington: The Science and Practice of Pharmacy* (Mack, Easton, PA, ed. 19, 1995).
28. H. Kawaguchi *et al*., *Biomaterials* **7**, 61 (1986); L. J. Krenis and B. Strauss, *Proc. Soc. Exp. Med.* **107**, 748 (1961); S. Rudt and R. H. Muller, *J. Controlled Release* **22**, 263 (1992).
29. P. Le Corre *et al*., *Int. J. Pharm.* **107**, 41 (1994).
30. M. Sacchetti and M. M. Van Oort, in (*3*), pp. 337–384.
31. J. W. Tom and P. G. Debenedetti, *J. Aerosol Sci.* **22**, 555 (1991).
32. J. Heyder *et al*., *ibid.* **17**, 811 (1986); D. A. Edwards, *ibid.* **26**, 293 (1995).

33. We thank J. Heidel and C. Perez de la Cruz for helpful technical assistance. Supported by an NSF CAREER Grant (D.E., J.M.) and NIH grants GM26698 (R.L.) and HD29125 (R.L., J.H.).

5 February 1997; accepted 8 May 1997